



# MID-AMERICA TRANSPORTATION CENTER

Report # MATC-KU: 465

Final Report  
25-1121-0001-465



## Properties of Fouled Railroad Ballast (Phase 1)

### Robert Parsons Ph.D., P.E.

Professor

Department of Civil, Environmental, and Architectural Engineering  
University of Kansas

### AJ Rahman

Graduate Research Assistant

### Jie Han, Ph.D., P.E.

Professor



2012

A Cooperative Research Project sponsored by the  
U.S. Department of Transportation Research and  
Innovative Technology Administration

The contents of this report reflect the views of the authors, who are responsible for the facts and the accuracy of the information presented herein. This document is disseminated under the sponsorship of the Department of Transportation University Transportation Centers Program, in the interest of information exchange.  
The U.S. Government assumes no liability for the contents or use thereof.

MATC

## **Properties of Fouled Railroad Ballast (Phase 1)**

AJ Rahman  
Graduate Research Assistant  
Department of Civil, Environmental and Architectural Engineering  
University of Kansas

Robert Parsons, Ph.D., P.E.  
Professor  
Department of Civil, Environmental and Architectural Engineering  
University of Kansas

Jie Han, Ph.D., P.E.  
Professor  
Department of Civil, Environmental and Architectural Engineering  
University of Kansas

A Report on Research Sponsored by

Mid-America Transportation Center

University of Nebraska-Lincoln

October 2012

## Tehcnical Report Documentation Page

1. Report No. 25-1121-0001-465	2. Government Accession No.	3. Recipient's Catalog No.	
4. Title and Subtitle Properties of Fouled Railroad Ballast (Phase 1)		5. Report Date October 2012	
		6. Performing Organization Code	
7. Author(s) AJ Rahman, Robert Parsons, and Jie Han		8. Performing Organization Report No. 25-1121-0001-465	
9. Performing Organization Name and Address Mid-America Transportation Center 2200 Vine St. PO Box 830851 Lincoln, NE 68583-0851		10. Work Unit No. (TRAIS)	
		11. Contract or Grant No.	
12. Sponsoring Agency Name and Address Research and Innovative Technology Administration 1200 New Jersey Ave., SE Washington, D.C. 20590		13. Type of Report and Period Covered July 2011 – June 2012	
		14. Sponsoring Agency Code MATC TRB RiP No. 24487	
15. Supplementary Notes			
<p>16. Abstract</p> <p>Ballasted tracks are the most common tracks used in the railroad industry and are designed to provide a stable, safe, and efficient rail foundation. A ballasted track consists of superstructure (ties, fasteners, and rails) and substructure (ballast, sub-ballast, and subgrade layers). The main functions of ballast are to support the superstructure by distributing the loads from the moving train, and to provide lateral resistance to tie movement and drainage. However, ballast deterioration and fouling are major issues in the railroad industry, and can be caused by repeated loadings, which lead to crushing ballast that is in contact with ties. Upward migration of subgrade particles into the ballast layer can increase fouling in the ballast and decrease drainage through the ballast layer. There is a need for methods to easily and inexpensively identify areas that have fouled ballast. The objective of this preliminary study was to evaluate the potential for estimating the level of fouling in a ballast layer by soil resistivity and permeability tests to be followed by a second study. A test box was designed and fabricated at the lab at the University of Kansas to perform the constant head permeability test and soil resistivity tests. Constant head tests were conducted to determine the coefficient of permeability of fouled ballast for different fouling percentages. Soil resistivity tests were also conducted using the Wenner method (4 point method) to determine the resistivity of ballast for different percentages of fouling. The tests showed a relationship between the percentage of fouling and ballast resistivity. The resistance of the ballast layer decreased as the percentage of fouling increased due to the presence of water. Fouled material retained water and filled the voids between the ballast particles, and therefore decreased resistivity in the ballast layer. The permeability (hydraulic conductivity) also decreased as the percentage of fouling increased due to the presence of fine particles between the ballast particles; therefore, permeability and resistivity were also correlated.</p>			
17. Key Words Ballast, fouling, resistivity, permeability		18. Distribution Statement	
19. Security Classif. (of this report) Unclassified	20. Security Classif. (of this page) Unclassified	21. No. of Pages 45	22. Price

## Table of Contents

Acknowledgments.....	vii
Disclaimer.....	viii
Abstract.....	ix
Chapter 1 Introduction.....	1
Chapter 2 Literature Review.....	3
2.1 Effects of Fouled Ballast.....	3
2.2 Soil Resistivity.....	4
2.3 Railroad Ballast Fouling Detection.....	6
Chapter 3 Material Testing.....	9
3.1 Material.....	9
3.1.1 Gradation of Ballast.....	9
3.1.2 Gradation of Crushed Ballast Fines.....	11
3.1.3 Gradation of Clay.....	13
3.1.4 Specific Gravity and Absorption of Ballast Coarse Aggregates.....	13
3.1.5 Specific Gravity of Crushed Ballast Aggregates.....	15
3.1.6 Specific Gravity of Clay.....	15
3.2 Summary.....	15
Chapter 4 Permeability and Resistivity of Fouled Ballast.....	17
4.1 Test Setup and Instrumentation.....	17
4.2 Test Procedure.....	22
Chapter 5 Results.....	32
5.1 Permeability Test Data.....	32
5.2 Resistivity Test Data.....	34
6.1 Permeability and Percentage Fouling.....	38
6.2 Resistivity and Percentage Fouling.....	40
Chapter 7 Conclusions and Future Work.....	43
References.....	44

## List of Figures

Figure 3.1 Sieve shaker .....	10
Figure 3.2 Gradation curves of the ballast aggregates .....	10
Figure 3.3 Gradation curve of the crushed ballast fines .....	12
Figure 3.4 Gradation curve of clay .....	13
Figure 3.5 Ballast aggregates immersed in water .....	14
Figure 3.6 Ballast aggregates in SSD condition .....	14
Figure 3.7 Wire basket and scale used to measure weight of aggregates when submerged in water .....	14
Figure 4.1 Plastic support and fiber glass screen .....	18
Figure 4.2 Cut front wall of the box and place the glass wall .....	19
Figure 4.3 Secure and seal glass wall .....	19
Figure 4.4 Aluminum sheets and copper rods spaced equally .....	20
Figure 4.5 Schematic diagram for the setup of the test .....	20
Figure 4.6 Schematic diagram for the setup of the test with dimensions .....	21
Figure 4.7 Picture of actual test setup .....	22
Figure 4.8 Washing the box prior to testing .....	24
Figure 4.9 Screen wrapped around support .....	24
Figure 4.10 Verify box is leveled .....	25
Figure 4.11 Tap sides of the wall to compact sample .....	25
Figure 4.12 First layer of ballast mixed with fouling material .....	25
Figure 4.13 Box filled with sample and ready for test .....	26
Figure 4.14 Flooding the sample with water through the bottom pipe .....	27
Figure 4.15 Water rise in standpipe relative to water level in sample .....	28
Figure 4.16 Close picture of height of water in standpipe .....	28
Figure 4.17 Constant head flow exiting the outflow pipe .....	29
Figure 4.18 Collect water at a certain time period .....	29
Figure 4.19 Verify draining water is clean (no loss of fines) .....	30
Figure 4.20 Aluminum sheets and copper rods connected to resistivity meter .....	30
Figure 4.21 Measure resistance in sample .....	31
Figure 5.1 Measured hydraulic conductivity versus percentage fouling for crushed ballast fines and clay .....	32
Figure 5.2 Measured hydraulic conductivity (log scale) versus percentage fouling for crushed ballast fines and clay .....	33
Figure 5.3 Measured resistivity of fouled ballast (crushed ballast fines) versus time at different percentages of fouling .....	34
Figure 5.4 Measured resistivity of fouled ballast (clay) versus time at different percentages of fouling .....	35
Figure 5.5 Measured resistivity of fouled ballast at the 18 <sup>th</sup> hour versus percentage fouling .....	36
Figure 5.6 Comparison between measured hydraulic conductivity and resistivity at 18 <sup>th</sup> hour versus percentage fouling .....	37
Figure 6.1 Hydraulic conductivity versus fouling index of fouled ballast .....	39

## List of Tables

Table 2.1 Typical resistivity values of some soils .....	5
Table 3.1 BNSF specification limits (class 1) .....	11
Table 3.2 Gradation data for crushed ballast fines .....	12
Table 3.3 Specific gravity of ballast coarse aggregates .....	15
Table 3.4 Properties of fouling materials .....	16
Table 3.5 Summary of grain size characteristics of ballast and fouling materials .....	16
Table 5.1 Hydraulic conductivity values for different percentages of ballast .....	33
Table 5.2 Measured resistivity range for each percentage of fouling for crushed ballast fines .....	35
Table 5.3 Measured resistivity range for each percentage of fouling for clay .....	36
Table 5.4 Comparison of the resistivity of fouled ballast (crushed ballast fines and clay) at the 18 <sup>th</sup> hour .....	37
Table 6.1 Categories of fouling based on percentage fouling and fouling index .....	39

## List of Abbreviations

BNSF Railway (BNSF)  
Ground Penetrating Radar (GPR)  
Liquid Limit (LL)  
Mid-America Transportation Center (MATC)  
Percentage Void Contamination (PVC)  
Time Domain Reflectometry (TDR)

## Acknowledgments

The authors thank the Mid-America Transportation Center (MATC) for providing financial support for the research described in this report, and Mr. Hank Lees of BNSF for providing material and technical support for this research. We also thank the many individuals who contributed to the completion of this research, including, Mrs. Jennifer Penfield, Mr. Jitendra Thakur, Mr. Deep Khatri, Mr. Raju Acharya and especially Mr. Jim Weaver and Mr. Matthew Maksimowicz for their help in with the physical testing.

## Disclaimer

The contents of this report reflect the views of the authors, who are responsible for the facts and the accuracy of the information presented herein. This document is disseminated under the sponsorship of the Department of Transportation University Transportation Centers Program, in the interest of information exchange. The U.S. Government assumes no liability for the contents or use thereof.

## Abstract

Ballasted tracks are the most common tracks used in the railroad industry and are designed to provide a stable, safe, and efficient rail foundation. A ballasted track consists of superstructure (ties, fasteners, and rails) and substructure (ballast, sub-ballast, and subgrade layers). The main functions of ballast are to support the superstructure by distributing the loads from the moving train, and to provide lateral resistance to tie movement and drainage. However, ballast deterioration and fouling are major issues in the railroad industry, and can be caused by repeated loadings, which lead to crushing ballast that is in contact with ties. Upward migration of subgrade particles into the ballast layer can increase fouling in the ballast and decrease drainage through the ballast layer. There is a need for methods to easily and inexpensively identify areas that have fouled ballast. The objective of this preliminary study was to evaluate the potential for estimating the level of fouling in a ballast layer by soil resistivity and permeability tests to be followed by a second study. A test box was designed and fabricated at the lab at the University of Kansas to perform the constant head permeability test and soil resistivity tests. Constant head tests were conducted to determine the coefficient of permeability of fouled ballast for different fouling percentages. Soil resistivity tests were also conducted using the Wenner method (4 point method) to determine the resistivity of ballast for different percentages of fouling. The tests showed a relationship between the percentage of fouling and ballast resistivity. The resistance of the ballast layer decreased as the percentage of fouling increased due to the presence of water. Fouled material retained water and filled the voids between the ballast particles, and therefore decreased resistivity in the ballast layer. The permeability (hydraulic conductivity) also decreased as the percentage of fouling increased due to the presence of fine particles between the ballast particles; therefore, permeability and resistivity were also correlated.

## Chapter 1 Introduction

A rail track structure is designed to provide a stable, safe, and efficient path for trains to operate at high speeds while transporting substantial loads. Ballasted track is the most common type of rail structure used throughout the world due to its relatively low cost of construction and maintenance (1). A ballasted track system usually consists of a superstructure (ties, fasteners and rails), and substructure (ballast, sub-ballast and subgrade layers) (2). Ballast consists of uniformly graded coarse aggregate placed between the cross ties and subgrade (3). The main functions of railroad ballast are to support the superstructure by distributing the loads from the moving train to provide lateral resistance, and to facilitate drainage. The physical properties of good, quality ballast can be classified by its angularity of particles, high toughness, high resistance to weathering, rough surface, high specific gravity, and shear strength (3).

Ballast deterioration and fouling are major issues in the railroad industry, and can be caused from repeated dynamic loading, vibration, temperature, and the presence of water. Fouling is caused by breakage of the ballast aggregate, spillage of coal dust from moving trains, and the migration of subgrade particles. As the percentage of fouling in the ballast and sub-ballast layers increases, more water is retained by the fouled layers, resulting in track instability due to the buildup of pore water pressure, as well as alignment problems. Detection of the percentage of fouling in ballast has been a challenging task for maintenance units, especially if the drainage capacity varies significantly beneath the track with location. Track maintenance divisions need to have a system for scheduling maintenance when needed in order to maintain safe operation and traffic flow.

The objective of this study was to obtain a proper understanding of the fouling of ballast caused by various types of fines, and its implications on track drainage, which can affect track

maintenance operations. Additionally, this study sought to determine the feasibility of evaluating the percentage fouling in railroad ballast by measuring the resistivity in the ballast and sub-ballast layer and finding a correlation between ballast permeability and resistivity. Tests included two main sources of fouling: internal ballast crushing and fine particles migrating from subgrade. A relationship between the resistivity of ballast and percentage fouling was observed. This was a preliminary study, with a more detailed study to be conducted in 2012-2013.

## Chapter 2 Literature Review

### 2.1 Effects of Fouled Ballast

As ballast ages, it becomes progressively fouled with fine material filling the voids between coarse particles. Several research studies report that around 70% of fouling material results from ballast aggregate breakage (3). Selig and Waters showed that about 76% of ballast fouling is caused by ballast breakdown, 13% by infiltration from sub-ballast, 7% by infiltration from the ballast surface, 3% from subgrade intrusion, and 1% is related to tie wear (5).

Raymond reported that the liquid limit (LL) of fine particles in the ballast layer should be less than 35 to function as a drainable layer; also showing that aggregate breakdown is mainly influenced by the physical properties of the mineral aggregate (6).

According to Indraratna, under saturated conditions water and fine particles mix to form slurry and will migrate to the sub-ballast and ballast layer. This migration can fill voids within coarse aggregates and decrease drainage, which may lead to ballast degradation and may cause serviceability problems with the superstructure. Ballast is designed to be a free drainage material with particle sizes ranging from 0.5 to 2.5 inches; however, the infiltration of fouling material reduces the void spaces and restricts drainage. Specifications for the gradation of ballast require a uniform gradation with a uniformity coefficient between 1.5 and 3. Fouling materials can have variable specific gravity, void ratio, and gradation, which will result in changing the characteristics of the ballast layer (3). In a study conducted by Wallace, an increase in the percentage of fines resulted in a decrease in hydraulic conductivity and decreased the drainage capacity of ballast; the results of the study showed that sand did not impact the permeability of ballast significantly; however, clay and silt caused a significant reduction on permeability of ballast (7).

Moreover, a study conducted by Chiang showed that ballast settlement increased with the percentage fouling in ballast (8). Han and Selig conducted a similar study where the results showed that the degree of ballast fouling had a significant impact on ballast settlement (9).

## 2.2 Soil Resistivity

Resistance is the ratio of applied voltage of the resulting current flow. Resistivity is the resistance of a conductor, which depends in its atomic structure and behavior of the material. The commonly used symbol for resistivity is  $\rho$ , and is usually measured in ohm-cm. the resistivity can be derived by the following equation:

$$\rho = (R \times A)/L \quad (2.1)$$

where,

R is resistance in ohms,

A is cross section area in  $\text{cm}^2$ ,

and L is length of conductor in cm.

A material with high resistivity is considered to be a bad conductor. Sand, loam, and crushed stone aggregate have high resistance and are considered to be bad conductors. However, when water is present, the resistivity decreases and the soil or aggregate will become a conductor, though still considered to be a poor conductor compared to metals. The resistivity of soil will be governed by the quantity of water held in the soil. In other words, conductivity of the soil would be a function of the water retained within the soil.

The main factors which determine resistivity are (10):

- 1- Type of soil
- 2- Chemical composition of salts dissolved in the contained water
- 3- Moisture content
- 4- Temperature
- 5- Grain size of the material and distribution of grain size
- 6- Closeness of packing and pressure

**Table 2.1** Typical resistivity values of some soils (10)

<b>Type of Soil</b>	<b>Resistivity in ohm-cm</b>
Loams, garden soil	500 - 5000
Clays	800 – 5000
Clay, sand and gravel mixtures	4000 - 25,000
Sand and gravel	6000 - 10,000
Slates, shale, sandstone	1000 - 50,000
Crystalline rocks	20,000 - 1,000,000

There are several types of soil resistivity measurements that can be used in the field and also for laboratory testing (soil box testing). According to Tagg, the Wenner-four probe (point) method is considered to be the most accurate method, compared to the 2 point and 3 point methods. The configuration of the Wenner-four probe method consists of four probes placed at equal distances from each other. A current is sent through the two outer electrodes (probes) and the voltage is measured between the two inner probes (10). The soil resistance is determined

using Ohm's law,  $R = V/I$ . The following formula is used to determine soil resistivity in accordance with the Wenner-four probe method:

$$\rho = 2\pi \times R \times D \quad (2.2)$$

where,

R= resistance in ohms and D = Distance between probes in cm (11).

Two other types of soil resistivity measurement methods are found in the AEMC instrument manual, which can be used to determine the soil resistivity using AEMC equipment. The 2 point method measures the resistance between two points. The 3 point method (Fall-of-Potential) is used to measure resistance to ground of auxiliary electrodes and grids. The measurement of ground resistance can only be obtained with specially designed test equipment. Most equipment uses the Fall-of-Potential voltage of alternating current circulating around auxiliary electrodes and a ground electrode under test (11).

### 2.3 Railroad Ballast Fouling Detection

In order to evaluate the need for maintenance to assure continued safe operations and to prevent any structure instability or drainage problems, several methods have been introduced to evaluate the percentage fouling of ballast. Selig and Waters proposed two methods to quantify the level of ballast fouling. The first method is the fouling index, which is the sum of the percent by weight of ballast sample passing the 4.75 mm sieve plus the percent passing the 0.075 mm sieve. The second method is the percentage of fouling, which is the ratio of the dry weight of the material passing the 9.5 mm sieve to the dry weight of total sample (5). Feldman and Nissen developed the percentage void contamination (PVC) parameter to show the effect of void

decrease in ballast as the ratio between the total volume of re-compacted fouling material (passing the 9.5 mm sieve) and the void volume between re-compacted ballast aggregates. This method determines the percentage of voids occupied by fouling material, but the gradation of fouling particles cannot be taken into account (9). Another method proposed by Indraratna is called relative ballast fouling ratio. It is a ratio between the solid volumes of fouling particles passing a 9.5 mm sieve and ballast particles being retained on a 9.5 mm sieve. In this equation, the mass of the ballast and the mass and specific gravity of the fouling material are needed to compute the ballast fouling ratio (10).

Traditionally, a destructive drilling method is used to evaluate the condition of ballast; however, this method is time consuming (9). Ground penetrating radar (GPR) has been used in the past for ballast evaluation. According to Roberts and Rudy, GPR has been utilized as a non-disturbing evaluation tool to evaluate railroad ballast and fouling level. GPR data is obtained on railroad ballast using 2 GHz horn antennas, and provides data that contain significant scattering energy from the void space in the clean ballast. The data from fouled ballast produce less scattering energy due to fewer void spaces in ballast layer (9). The GPR method shows it is applicable for determining the percentage fouling in the ballast and sub-ballast layer; however, more data and ground properties are required to evaluate the limitations of this methodology (9). According to many previous studies, GPR is effective, and has been utilized to determine ballast conditions. According to Leng and Al Qadi, there are limitations that must be emphasized to ensure reliable results (11). First, the dielectric constant of the railroad ballast is unknown in many evaluation cases. Another limitation with the GPR method is that the signal reflection can only detect an interface where there is a significant difference in dielectric contrast properties, even though the gradation of ballast changes with depth and there may not be a clear interface

between fouled and clean ballast. Therefore, GPR may not be able to detect fouled ballast under certain conditions, which may lead to unreliable results (11).

Moreover, as the fouling level increases in a ballast layer, the reflection becomes less defined and data will be difficult to interpret. Overall, GPR studies illustrate the difficulty of data interpretation and the sensitivity of water content in fouled ballast (12).

Another study conducted by Ebrahimi (12) showed a method that detects and quantifies the fouling content by electromagnetic surveying and visual observation through boreholes. A small scale study was conducted using time domain reflectometry (TDR) to evaluate the change of electromagnetic parameters in detecting fouling content. The study focused on characterizing EM parameters of two main sources of fouled ballast, deteriorated ballast and coal dust, using the TDR methodology to assess the percentage fouling and moisture content. The test results showed that an increase in water content of the fouling material from 5 to 10% increased the electrical conductivity of ballast from 10 to 24mS/m. Ebrahimi's study also showed that the fouling content and water content increased the plastic deformation of the track (12).

## Chapter 3 Material Testing

This chapter contains descriptions of the railroad ballast, crushed ballast and clay, and the methods used to characterize them. The proposed tests ensure that the material meet the requirements to be used in the field.

### 3.1 Material

The railroad ballast material was provided by BNSF and was excavated from track undergoing maintenance in Gardner, Kansas. This material was characterized during a previous project (14). Several tests were conducted to determine the properties of ballast, crushed ballast, and clay in the soils lab at the University of Kansas.

#### *3.1.1 Gradation of Ballast*

The ballast coarse aggregates were separated by conducting a sieve analysis test, where the distribution of particle size was determined. Ballast aggregates were sieved with a sieve machine provided by BNSF, as shown in figure 3.1. Separation was achieved from retained particles of different sieve sizes starting at 2.5” opening and ending at 0.5.” The results of this test were plotted on a graph, as shown in figure 3.2, and the following parameters were determined: the maximum size, minimum size, coefficient of curvature, and coefficient of uniformity of ballast aggregates. The results were used to determine compliance of the particle size distribution with applicable specifications requirements provided by BNSF (table 3.1).



**Figure 3.1** Sieve shaker

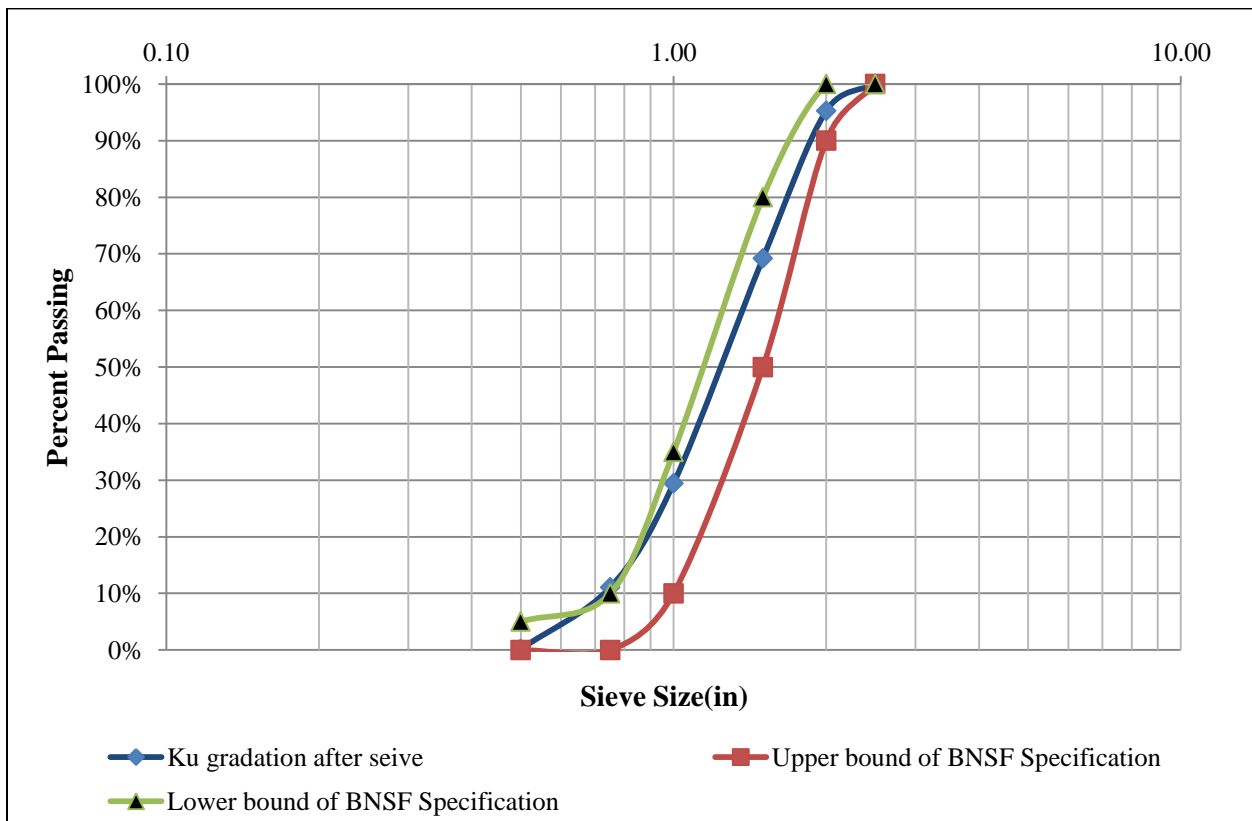


**Figure 3.2** Gradation curves of the ballast aggregates (14)

**Table 3.1** BNSF specification limits class 1 (14)

<b>Sieve Analysis (ASTM C 136)</b>	
<b>Sieve Size</b>	<b>BNSF Specification Limits (Class 1)</b>
2.5"	100
2"	90-100
1.5"	50-80
1"	10-35
0.75"	0-10
0.5"	0-5

### *3.1.2 Gradation of Crushed Ballast Fines*

The ballast fine aggregates were separated by sieve analysis, where the distribution of particle size was determined by sieving. This test separated the particles by their size. Separation was achieved for retained particles of different sieve sizes starting at 4.75 mm opening and ending at 0.075 mm, in accordance with ASTM D5444-08. The results of this test are plotted in figure 3.3. The maximum size, mean size, coefficient of curvature, and coefficient of uniformity of crushed ballast particles were found to be 9.5 mm, 1.7 mm, 0.959, and 7.19, respectively.

**Table 3.2** Gradation data for crushed ballast fines

Sieve No.	Size Opening (mm)	Mass Clean Sieve, Ms (g)	Mass Sieve and Soil, Mss (g)	Mass Retained, Mn (g)	% of mass retained	Cumulative % Retained	% Finer
4	4.75	498.77	734.87	236.1	18.4	18.4	<b>81.6</b>
8	2.36	477.94	736.24	258.3	20.1	38.5	<b>61.5</b>
16	1.18	442	726.56	284.56	22.1	60.6	<b>39.4</b>
30	0.6	400.56	626.53	225.97	17.6	78.2	<b>21.8</b>
50	0.3	368.33	533.3	164.97	12.8	91.0	<b>9.0</b>
100	0.15	341	411.8	70.8	5.5	96.6	<b>3.4</b>
200	0.075	326.24	352.4	26.16	2.0	98.6	<b>1.4</b>
Pan		496.07	512.87	16.8	1.4	100.0	<b>0.0</b>

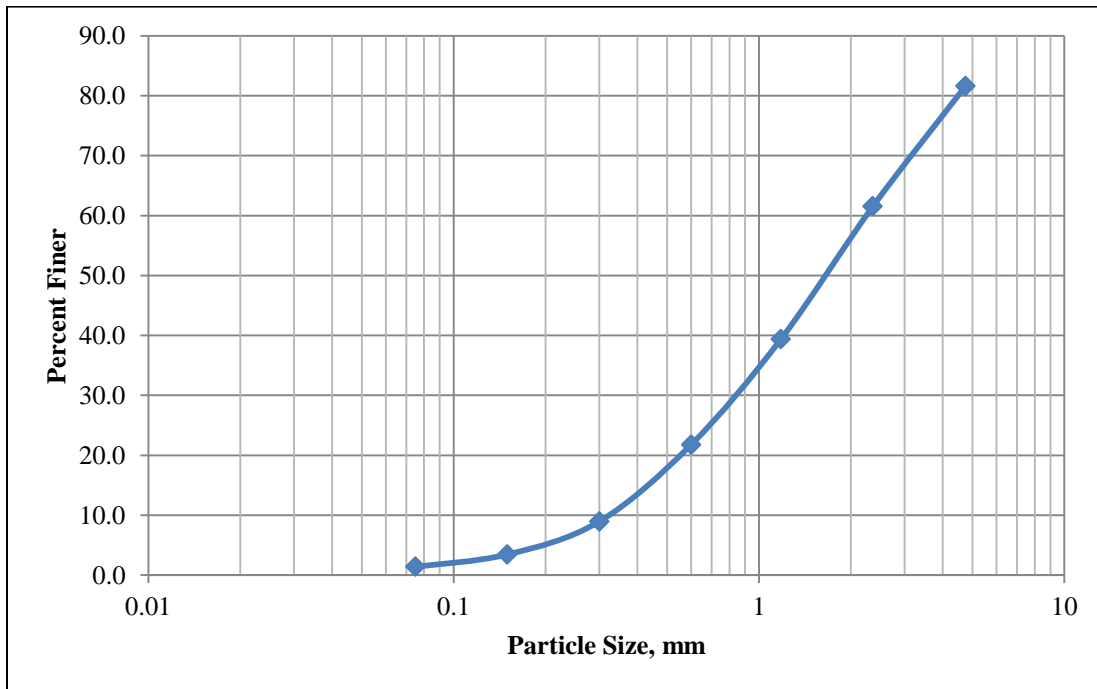


**Figure 3.3** Gradation curve of the crushed ballast fines

### 3.1.3 Gradation of Clay

The grain size distribution of the clay used as fouling material was determined by hydrometer analysis in accordance with ASTM D22.2703-1. The grain size distribution chart of the clay is shown in figure 3.4.



**Figure 3.4** Gradation curve of clay (14)

### 3.1.4 Specific Gravity and Absorption of Ballast Coarse Aggregates

This test method determines the average density of a quantity of coarse aggregate particles, the specific gravity, and the absorption of coarse aggregates. A sample of aggregates is immersed in water for 24 hours to essentially fill the pores. Then the sample is weighed after it is removed from the water and the surfaces of the particles are towel dried. Next, the sample is submerged in water and weighed. Finally, the sample is oven-dried and weighed for final dry mass. Using the mass values and the formulas provided by the test method will result in

obtaining the specific gravity and absorption of the aggregate. This test method was performed in accordance to ASTM C127. Pictures of the test are shown in figures 3.5 through 3.7. Specific gravity was used in calculating void content of aggregates and volume weight conversion. Table 3.3 shows the specific gravity of the ballast coarse aggregates.



**Figure 3.5** Ballast aggregates immersed in water



**Figure 3.6** Ballast aggregates in SSD condition



**Figure 3.7** Wire basket and scale used to measure weight of aggregates when submerged in water

**Table 3.3** Specific gravities of ballast coarse aggregates

Bulk Specific Gravity	2.72
SSD Bulk Specific Gravity	2.74
Apparent Specific Gravity	2.76
Absorption	0.54%

*3.1.5 Specific Gravity of Crushed Ballast Aggregates*

The specific gravity of crushed ballast was determined by the specific gravity of soil solids by water pycnometer test, in accordance with ASTM D854-06. The specific gravity was determined to be 2.61.

*3.1.6 Specific Gravity of Clay*

The specific gravity of clay was determined by the specific gravity of soil solids by water pycnometer test, in accordance with ASTM D854-06. The specific gravity was determined to be 2.74.

3.2 Summary

The properties of the ballast and fouling materials are shown in tables 3.4 and 3.5:

**Table 3.4** Properties of fouling materials

Fouling Material	LL (%)	PL (%)	Specific Gravity	Passing No. 200 Sieve (%)
Crushed Ballast	NA	NA	2.61	1.4
Clay	52	31	2.74	50

**Table 3.5** Summary of grain size characteristics of ballast and fouling material

	$D_{ave}$ (mm)	$D_{max}$ (mm)	Cc	Cu
Ballast	33	63.5	0.89	2
Crushed Ballast	1.7	9.5	0.959	7.19
Clay	0.075	0.1	NA	NA

## Chapter 4 Permeability and Resistivity of Fouled Ballast

This section includes descriptions of the test setups used for examining the permeability and resistivity of fouled ballast. Two sets of tests were performed; one using crushed ballast as the fouling material and one using clay, with different percentages of each material added to the ballast.

### 4.1 Test Setup and Instrumentation

For each fouling material four tests were conducted to examine the permeability and resistivity at different fouling levels. Constant head permeability tests were performed at the beginning of each test to determine the hydraulic conductivity of the sample. The same sample was then tested for resistivity with respect to time using a resistivity meter, in accordance with the Wenner 4 point method. The box was designed and fabricated at the geotechnical laboratory at the KU Civil, Environmental, and Architectural Engineering (CEAE) Department. The outside dimensions of the box were 42"x 29"x 28," and the inside dimensions were 39"x 26" x 22". Two layers of plastic support were placed at the bottom of the box and wrapped with fiberglass screen to prevent fines from going through, as shown in figure 4.1. The height of a typical sample was approximately 12." The front of the box was cut and replaced with a clear glass wall to permit visual observation, as shown in figures 4.2 and 4.3. A 2" pipe and valve were installed at the bottom of the box, which were used to fill the box with water and drain water out after the test. A 2" pipe was also installed at the back side of the box near the top to allow a constant water outflow. A 1" diameter plastic standpipe was also clamped and suspended freely beneath the fiberglass screen, used to measure the water level in the box during a test. Two sheets of aluminum were attached to the side walls of the box and two copper rods were held by clamps at equal distances of 13" from the side wall of the box, as shown in figure 4.4. The soil resistivity meter measured the resistivity within the sample by connecting all four electrodes to the meter. A

schematic diagram of the final setup is shown in figures 4.5 and 4.6. Figure 4.7 shows an actual test sample.

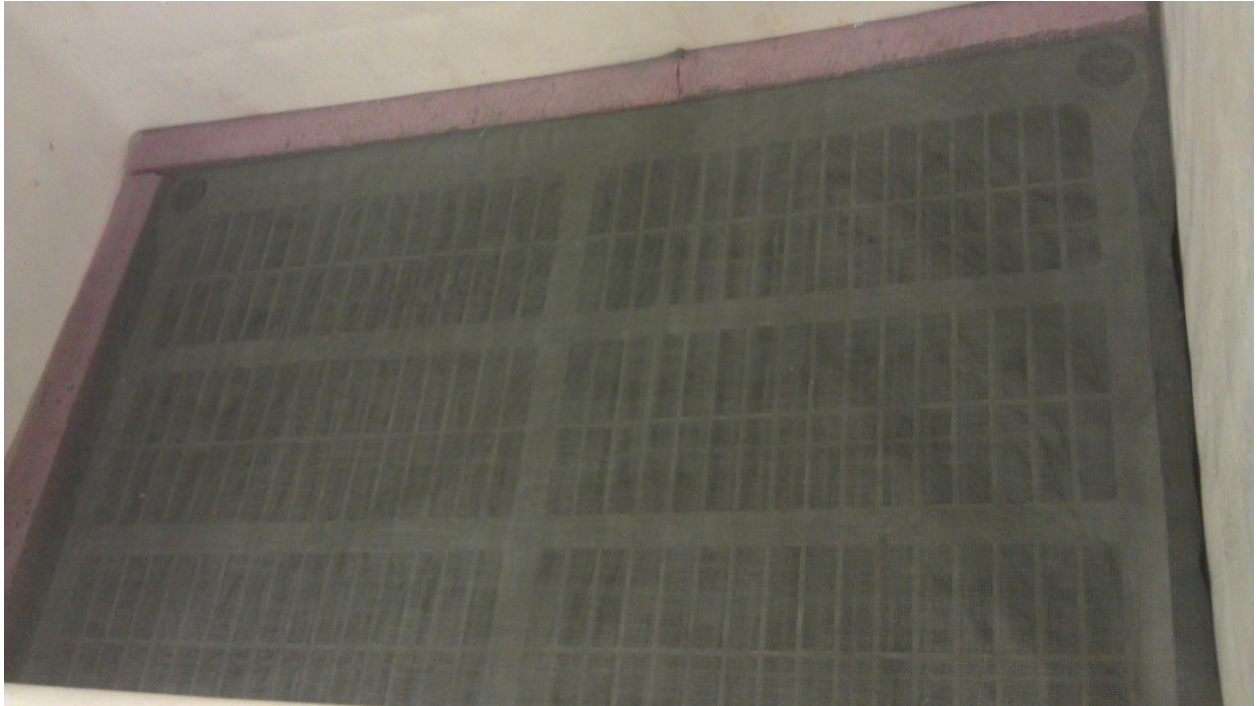


**Figure 4.1** Plastic support and fiber glass screen



**Figure 4.2** Cut front wall of the box and place the glass wall

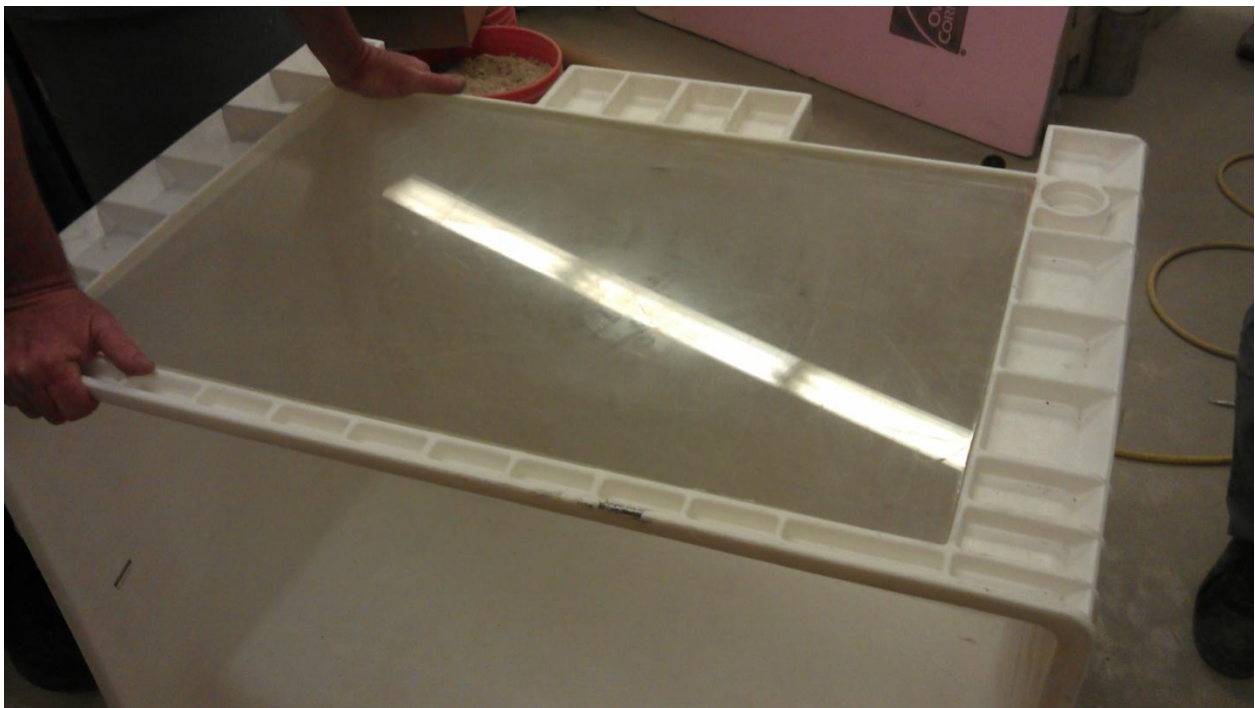


**Figure 4.3** Secure and seal glass wall

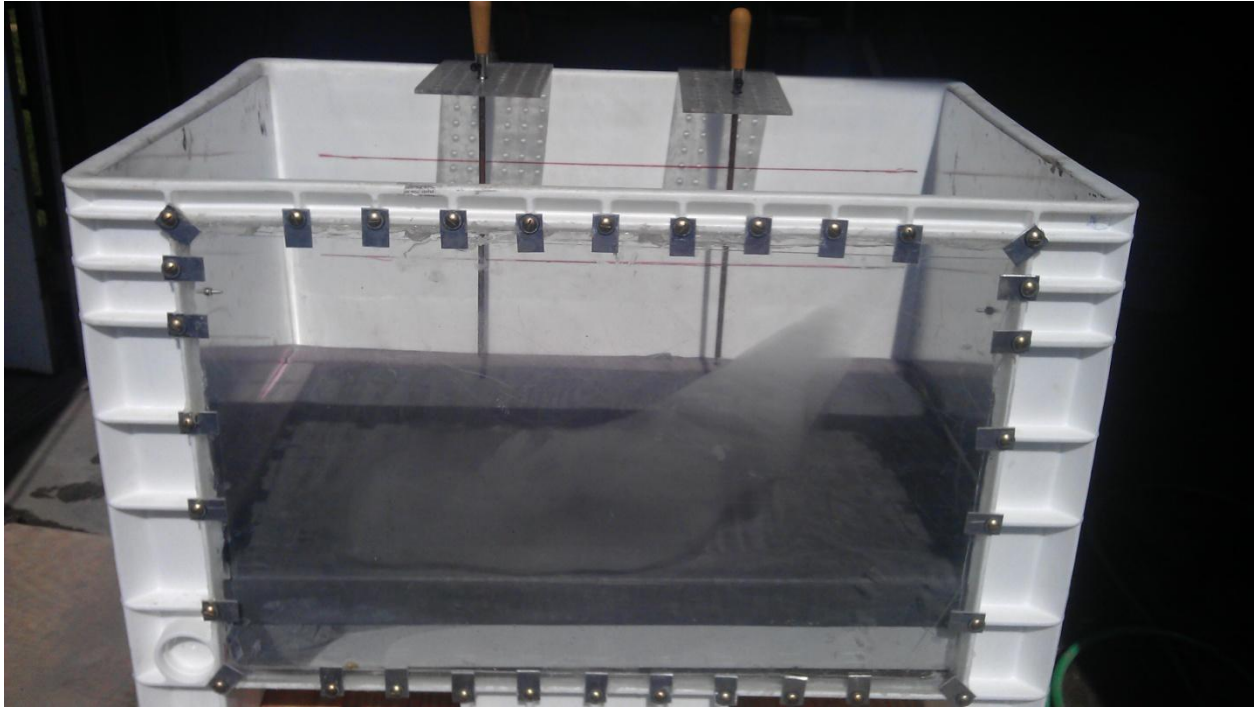


**Figure 4.4** Aluminum sheets and copper rods spaced equally

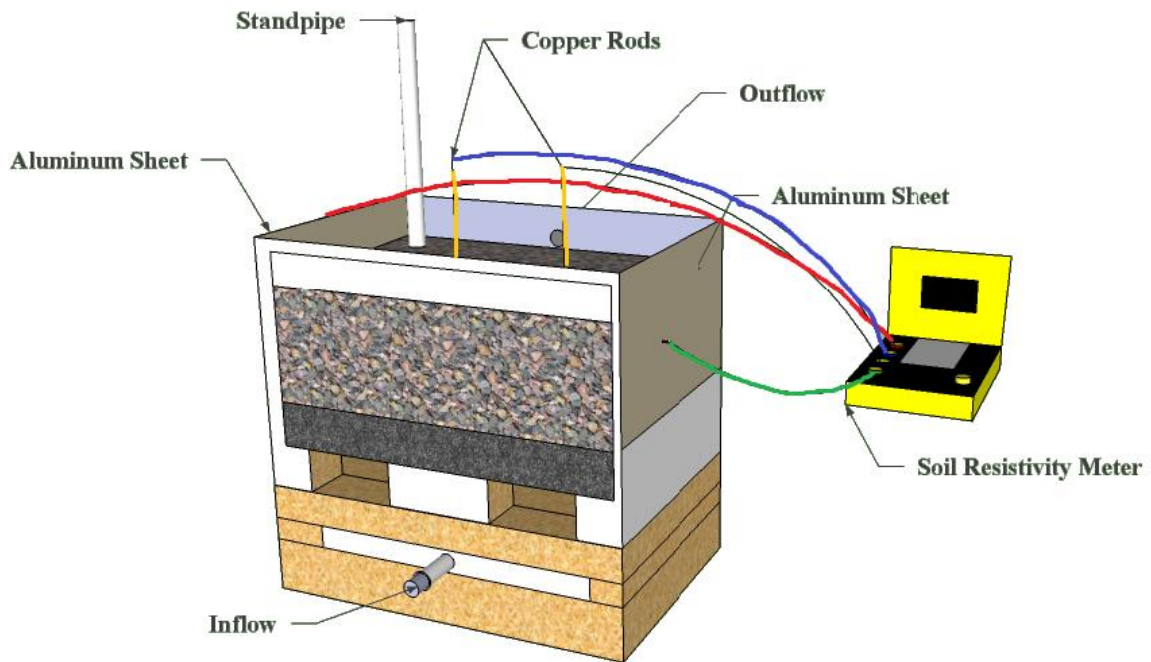


**Figure 4.5** Schematic diagram for the setup of the test

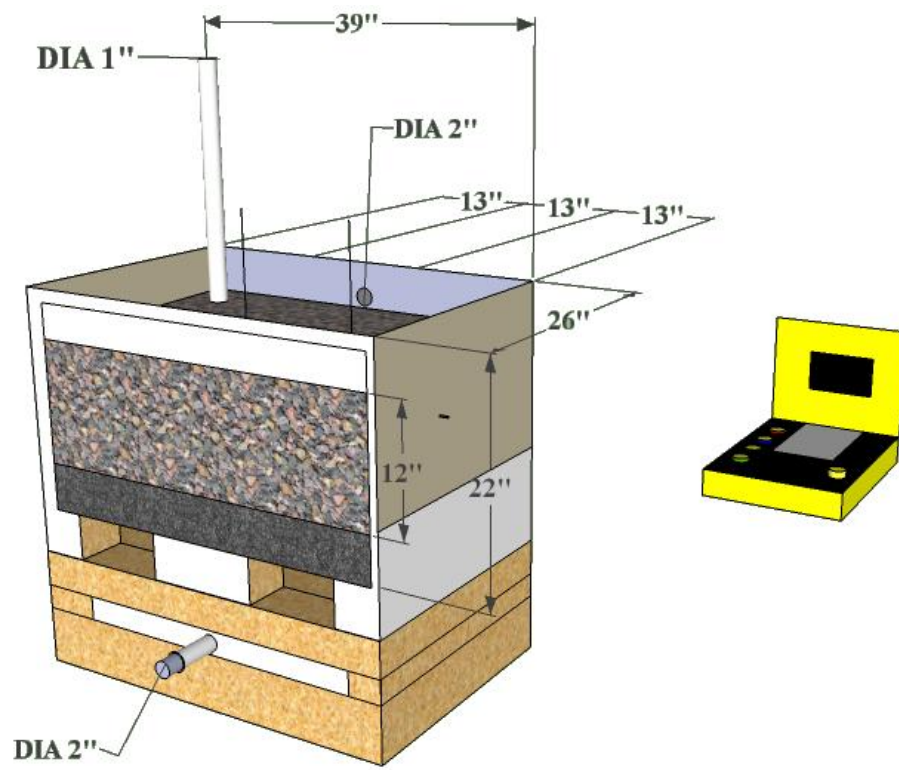


**Figure 4.6** Schematic diagram for the setup of the test with dimensions



**Figure 4.7** Picture of actual test setup

#### 4.2 Test Procedure

This section contains a description of the procedures followed for both the permeability and resistivity tests. First, the box was washed after every test to clean the residue from the previous test. The copper rods, aluminum sheets, standpipe, and screen were also cleaned before setting up for the next test. Then the fiberglass screen was fastened securely on the plastic support and around the corners of the box to prevent fines from migrating around the screen, which was necessary to obtain accurate results for the resistivity test. The box was then checked for level to make sure it was standing on a flat surface. Then, the sample, which consisted of ballast and the fouling material, was added to the box layers and spread out uniformly around the box. The sample was then compacted by tapping the walls of the box with a rubber mallet. The

hose was connected to the inflow pipe at the bottom of the box and water was introduced into the sample. A steady state flow condition (constant head) was established as water entered the lower reservoir, passed upward through the sample and into the upper reservoir, and exited through the outflow port. Water was collected from the upper reservoir (outflow) for a measured time period, and the mass and time were recorded. This procedure was repeated twice more before constant head flow was calculated. Constant head flow,  $Q$ , was determined by the following equation:

$$Q = \frac{M_w}{t \times \rho_w} \quad (4.1)$$

where,

$M_w$  = weight of water collected (g)

$t$  = measured time period (s)

$\rho_w$  = density of water, use 1 g/cm.<sup>3</sup>

For each test the height of the water rise was measured in the standpipe relative to the water level in the sample. Hydraulic conductivity was determined by the following equation:

$$k = \frac{QL}{\Delta h A} \quad (4.2)$$

where,

$L$  = length of sample (cm)

$A$  = area of sample (cm<sup>2</sup>)

$\Delta h$  = height of water rise in the standpipe.

The electrodes were then connected to the resistivity meter in order to take resistance readings, in accordance with the Wenner 4 point method, as the water drained out from the bottom pipe. The aluminum sheet on the east wall of the box was connected to X in the resistivity meter, the first copper rod was connected to Xv, the second copper rod was connected to Y, and the aluminum sheet on the west wall of the box was connected to Z. The four electrodes were set at equal distances from each other. A current was then passed through the outer electrodes, and the voltage between the two copper rods was measured. The soil resistance was measured by the resistivity meter, and the resistivity of the sample,  $\rho$ , was determined using equation 4.3. Time was recorded for each reading taken up to 24 hours.

$$\rho = 2\pi \times R \times A \quad (4.3)$$

Figures 4.8 through 4.21 present different steps taken to prepare the test:



**Figure 4.8** Washing the box prior to testing



**Figure 4.9** Screen wrapped around support



**Figure 4.10** Verify box is level



**Figure 4.11** Tap sides of the wall to compact sample



**Figure 4.12** First layer of ballast mixed with fouling material



**Figure 4.13** Box filled with sample and ready for test



**Figure 4.14** Flooding the sample with water through the bottom pipe



**Figure 4.15** Water rise in standpipe relative to water level in sample

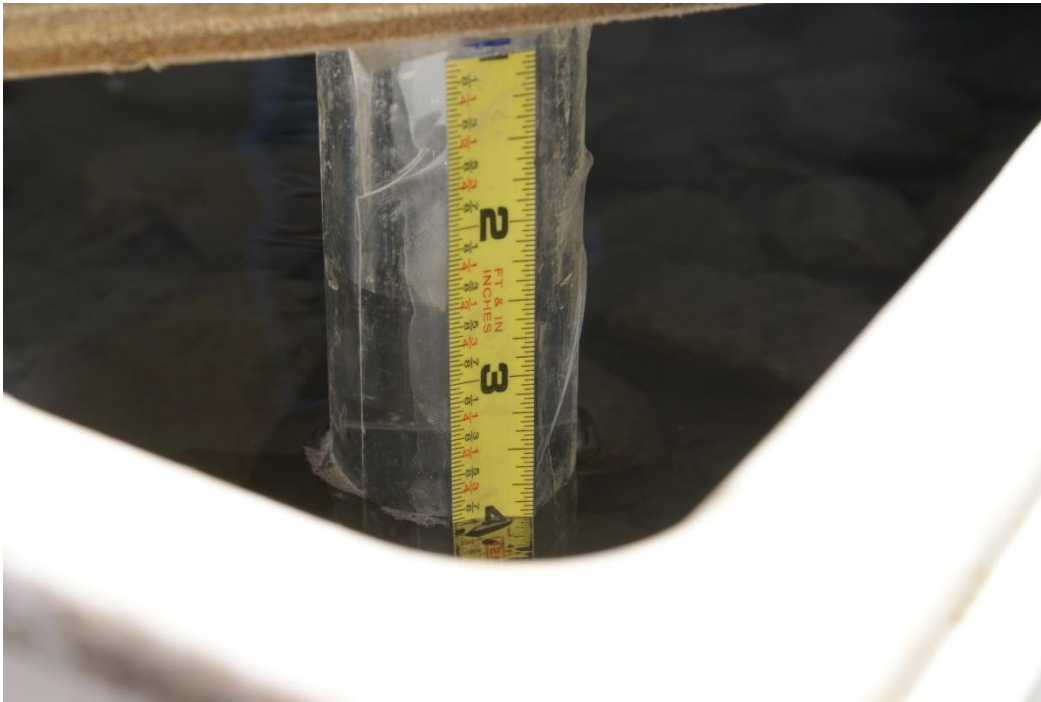


**Figure 4.16** Close picture of height of water in standpipe



**Figure 4.17** Constant head flow exiting the outflow pipe



**Figure 4.18** Collect water at a certain time period



**Figure 4.19** Verify draining water is clean (no loss of fines)



**Figure 4.20** Aluminum sheets and copper rods connected to resistivity meter

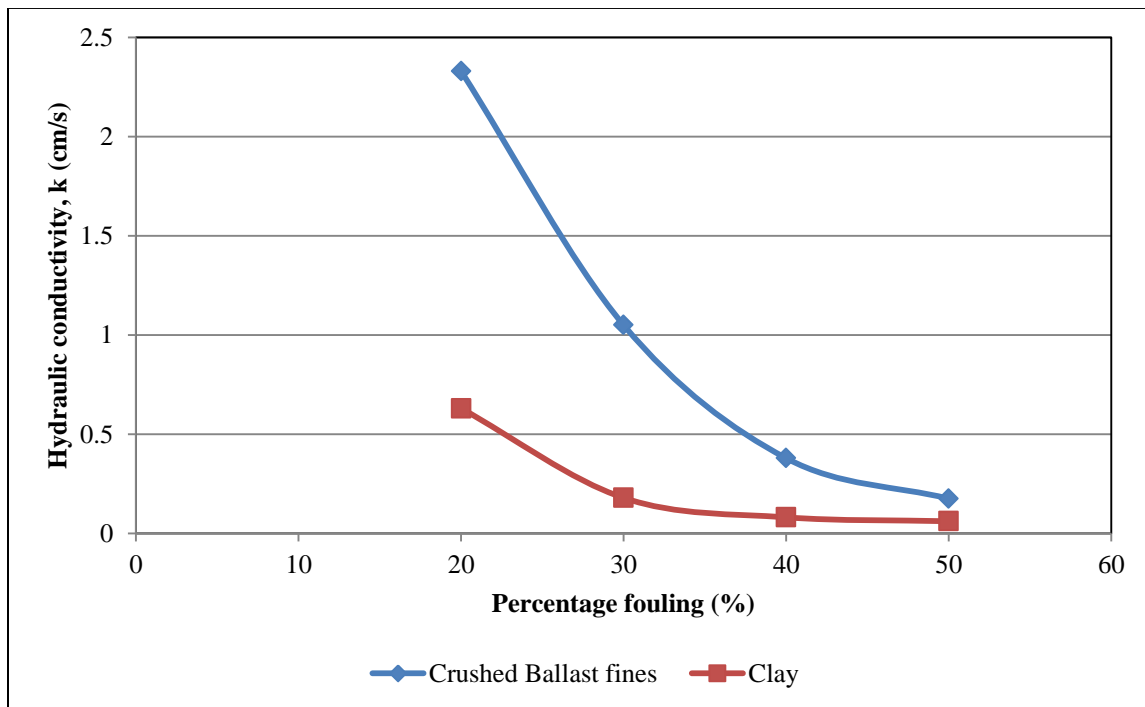


Figure 4.21 Measure resistance in sample

## Chapter 5 Results

### 5.1 Permeability Test Data

Four constant head permeability tests were conducted for each fouling material. Samples were prepared at 20, 30, 40, and 50 percent fouling. According to Selig and Waters, the percentage of fouling is the ratio of the dry weight of fouled material passing the 9.5mm sieve to the total weight of dry fouled ballast (5). Figures 5.1 and 5.2 show the relationship of hydraulic conductivity with percentage fouling for crushed ballast fines and clay on an arithmetic and logarithmic scale. The hydraulic conductivity was calculated using equation 4.2, and the results are presented in table 5.1.



**Figure 5.1** Measured hydraulic conductivity versus percentage fouling for crushed ballast fines and clay

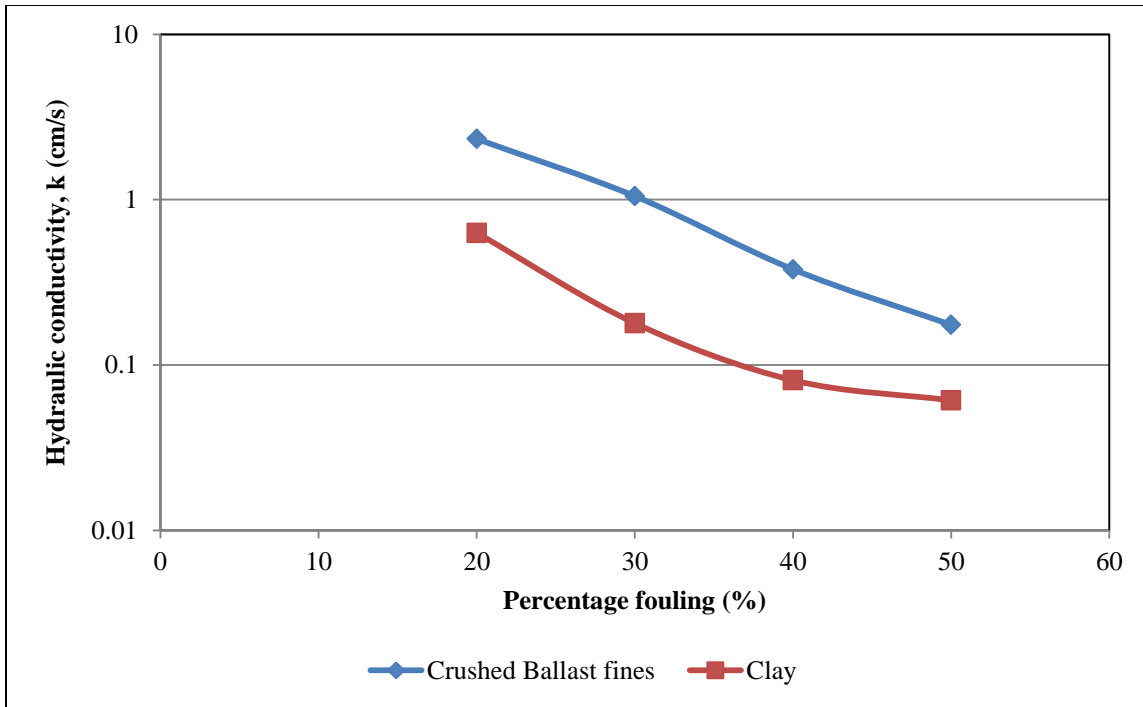


**Figure 5.2** Measured hydraulic conductivity (log scale) versus percentage fouling for crushed ballast fines and clay

**Table 5.1** Hydraulic conductivity values for different percentages of fouling for crushed ballast

<b>Permeability Test</b>		
<b>Percentage of fouling</b>	<b>Hydraulic Conductivity with Crushed ballast, k (cm/s)</b>	<b>Hydraulic Conductivity with Clay, k (cm/s)</b>
20%	2.33	0.63
30%	1.05	0.179
40%	0.379	0.0809
50%	0.175	0.0611

## 5.2 Resistivity Test Data

For each sample, a resistivity test was conducted at different time intervals up to 24 hours. As the water drained out of the sample, resistance readings were taken at recorded time periods to develop a range for each fouling material and the percentage fouling. Figures 5.3 and 5.4 show the relationship of resistivity of fouled ballast (both crushed ballast and clay) with time at 20, 30, 40 and 50 percent fouling. Also, tables 5.2 and 5.3 show the resistivity range for each percentage of fouling of both crushed ballast fines and clay. Figure 5.5 shows the resistivity for each test at the 18<sup>th</sup> hour measurement. Table 5.4 shows the actual resistivity measurement comparison for the fouled ballast with crushed ballast fines and clay at the 18<sup>th</sup> hour. Figure 5.6 shows the hydraulic conductivity and resistivity plotted versus percentage fouling.

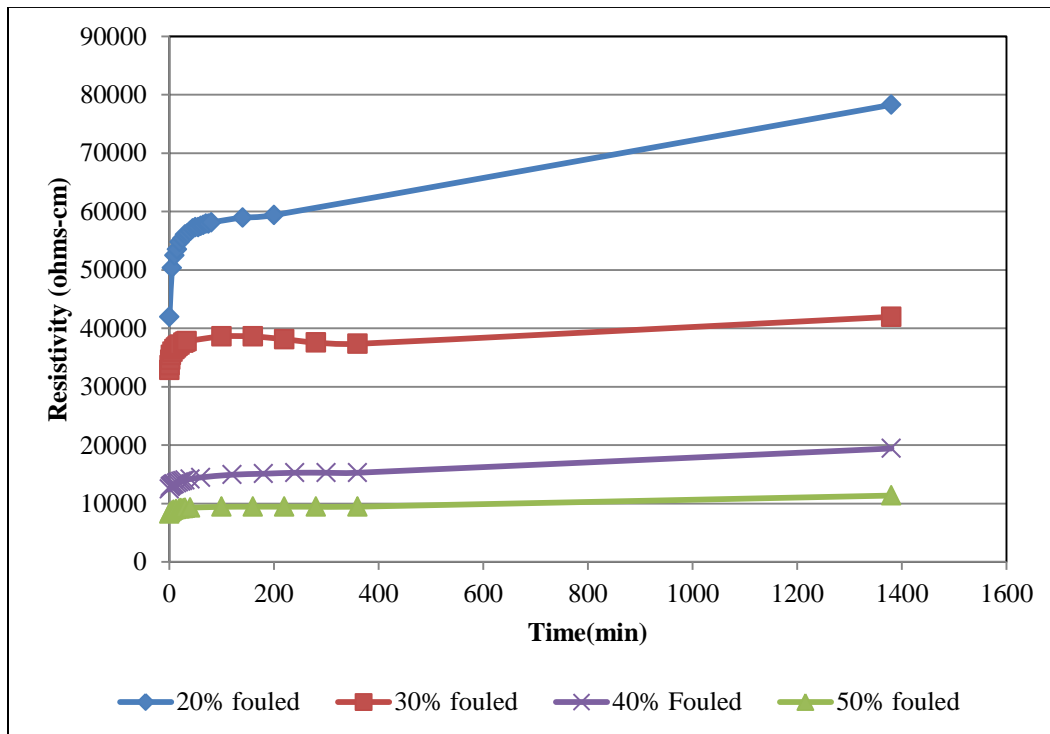


**Figure 5.3** Measured resistivity of fouled ballast (crushed ballast fines) versus time at different percentages fouling

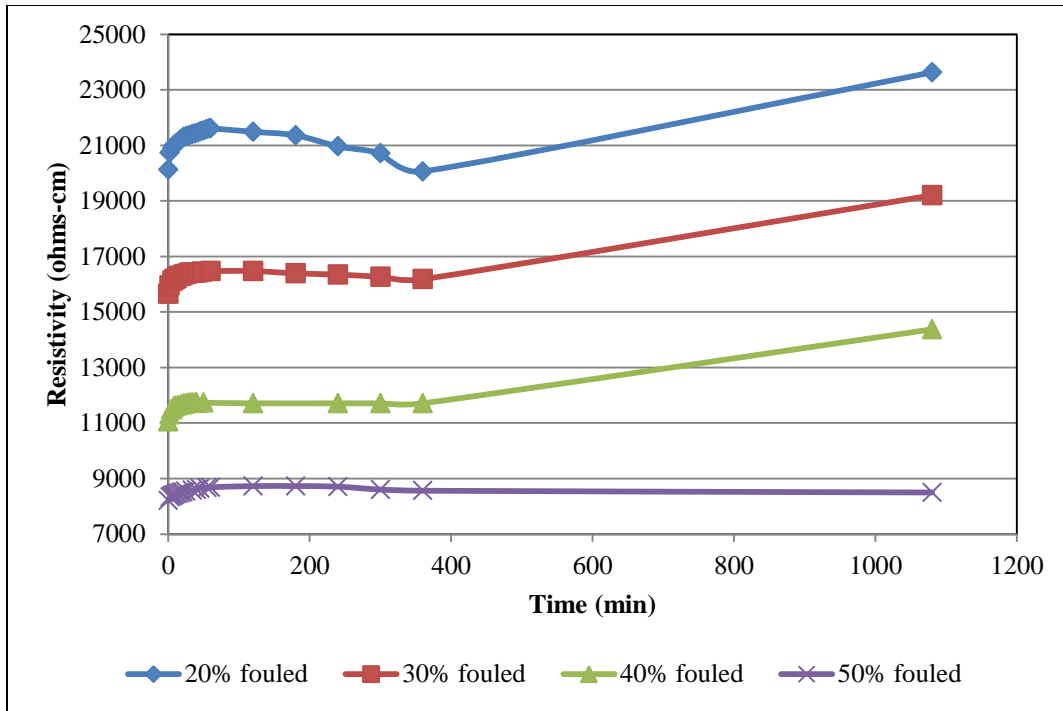


**Figure 5.4** Measured resistivity of fouled ballast (clay) versus time at different percentages of fouling

**Table 5.2** Measured resistivity range for each percentage of fouling for crushed ballast fines

<b>Crushed Ballast</b>	
<b>Percentage Fouling</b>	<b>Resistivity (ohms-cm) Range</b>
20%	42,000 - 80,000
30%	32,000 - 42,000
40%	12,000 - 20,000
50%	8,000 - 12,000

**Table 5.3** Measured resistivity range for each percentage of fouling for clay

Clay	
Percentage Fouling	Resistivity (ohms-cm) Range
20%	20,000 - 24,000
30%	15,000 - 20,000
40%	11,000 - 15,000
50%	8,000 - 9,000

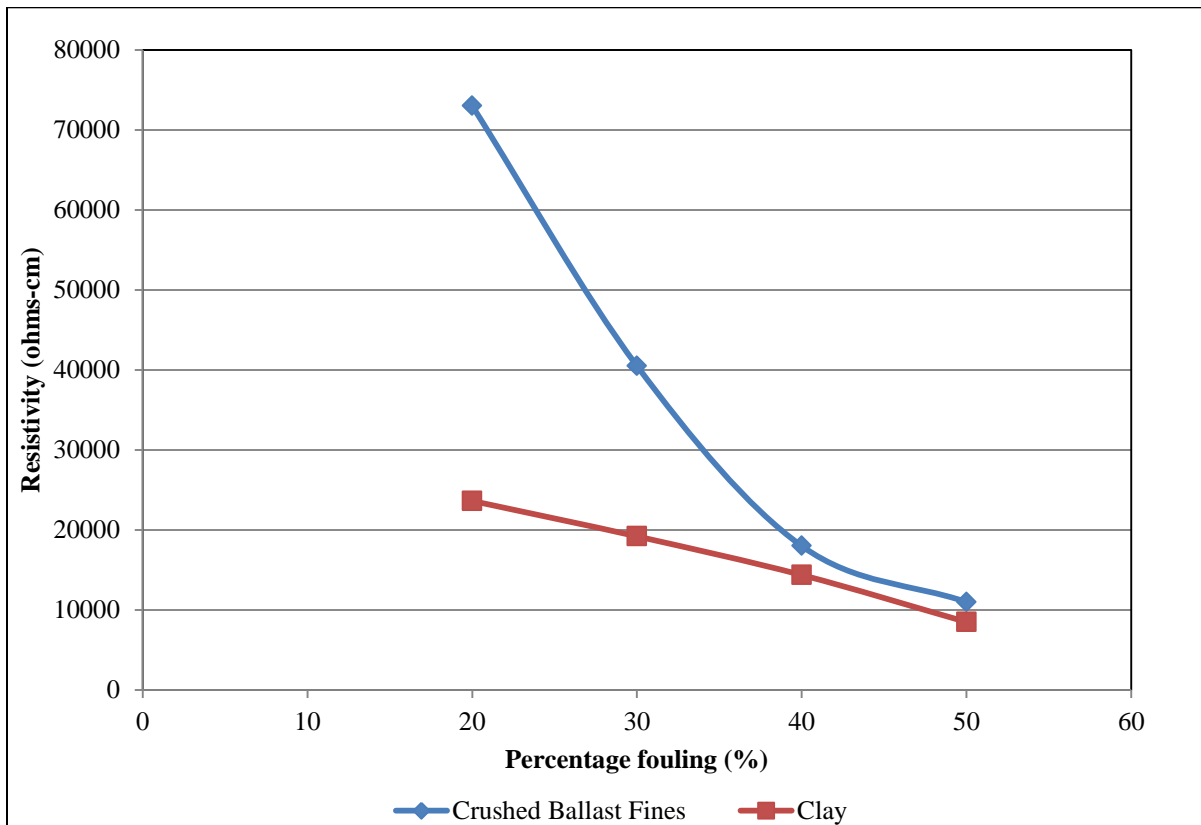


**Figure 5.5** Measured resistivity of fouled ballast at the 18<sup>th</sup> hour versus percentage fouling

**Table 5.4** Comparison of the resistivity of fouled ballast (crushed ballast fines and clay) at the 18<sup>th</sup> hour

Percentage fouling	Resistivity (ohms- cm)	
	Crushed ballast	Clay
20%	73,000	23,630
30%	40,500	19,202
40%	18,000	14,375
50%	11,000	8,499

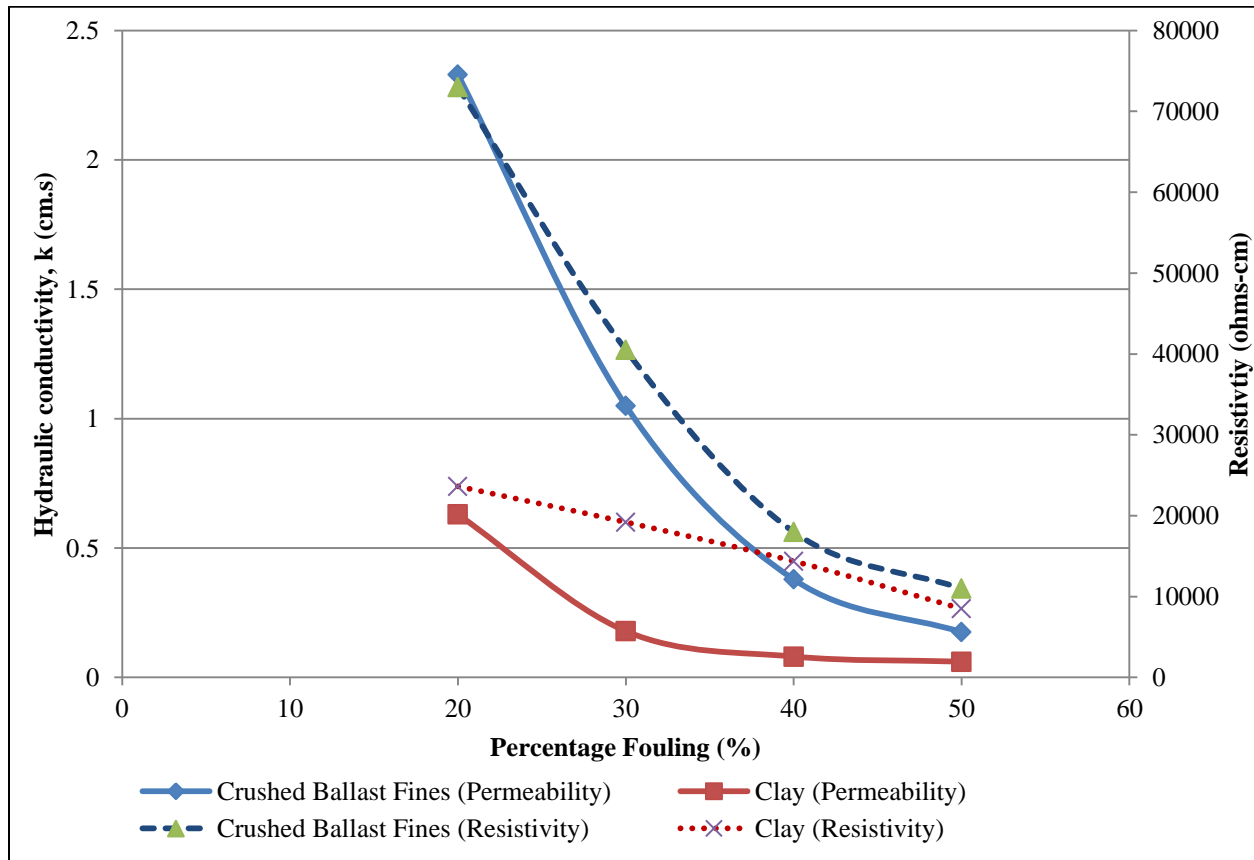


**Figure 5.6** Comparison between measured hydraulic conductivity and resistivity at 18<sup>th</sup> hour versus percentage fouling

## Chapter 6 Discussion

### 6.1 Permeability and Percentage Fouling

The relationships between permeability and percentage fouling are shown in table 5.1 and figure 5.1. The results confirm that permeability decreases substantially when the percentage of fouling increases, as fines fill up the voids between ballast coarse aggregates and restrict flow. Figures 5.1 and 5.2 show a sharp decrease in permeability as the percentage fouling increased for both crushed ballast and clay, with permeability for the ballast fouled with clay consistently below that of ballast fouled with crushed ballast particles. Size distribution played a major role in the comparison between crushed ballast and clay particles. The clay grain size distribution curve shows that more 50% of the clay particles passed the No. 200 sieve compared to 1.4% of crushed ballast particles.

Figure 6.1 presents the hydraulic conductivity versus fouling index of fouled ballast with crushed ballast fines and clay. The fouling index was proposed by Selig and Waters (5), and is represented by the sum of the percentages that passed the No. 4 sieve and the No. 200 sieve. The fines that passed the No. 200 sieve are accounted for twice in this index due to the significance of the size of fine particles in decreasing the drainage capacity. Plotting of fouling using the fouling index resulted in similar hydraulic conductivity values for different materials with the same fouling index. The fouling index adjusts for the different grain size distribution, and was therefore less dependent on fouling material type.

According to Indraratna (2), and as shown in table 6.1, the ballast layers are considered highly fouled when the percentage of fouling is greater than 34%, or a fouling index of 40% or greater.

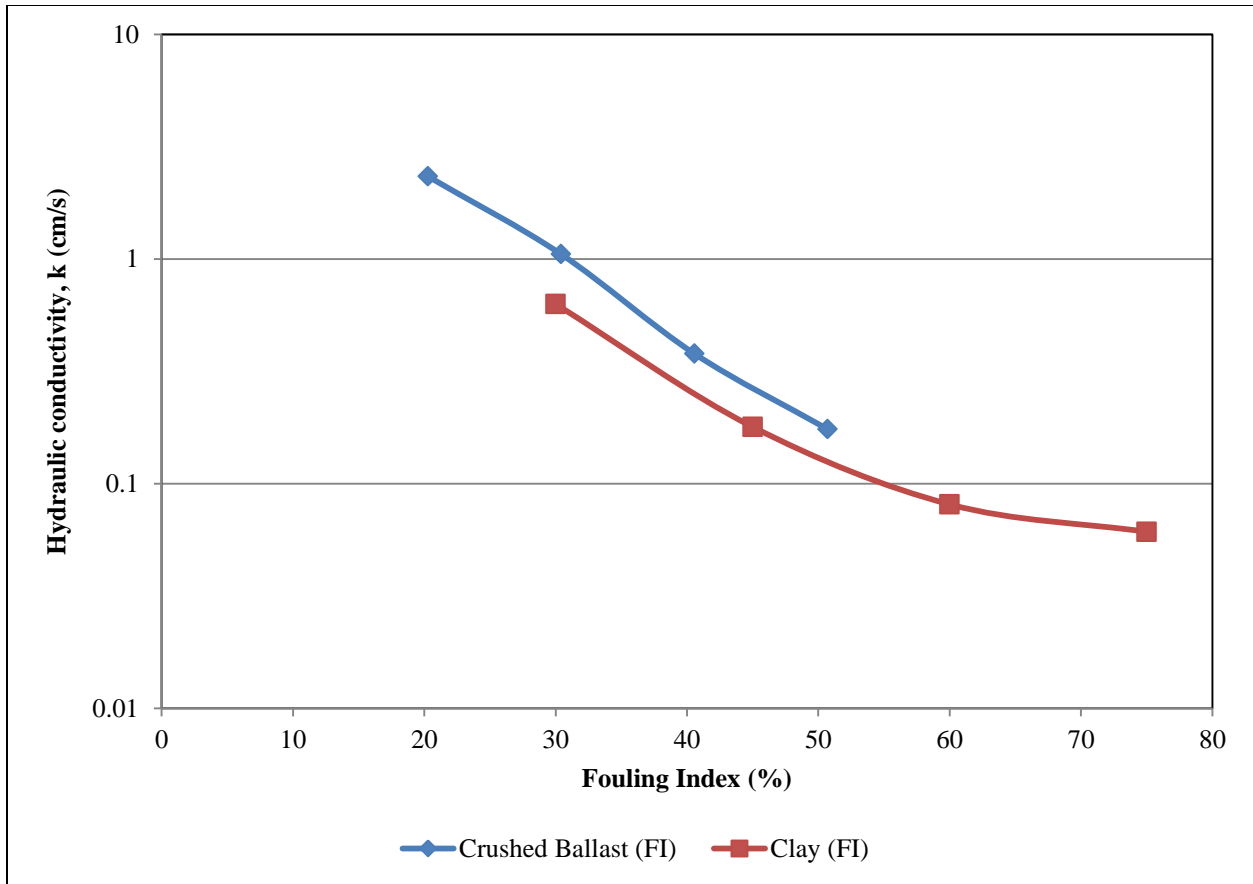


**Figure 6.1** Hydraulic conductivity versus fouling index of fouled ballast

**Table 6.1** Categories of fouling based on percentage fouling and fouling index (1)

Category	Percentage of fouling (%)	Fouling Index (Selig and Waters) (%)
Clean	< 2	< 1
Moderately clean	2 to < 9.5	1 to < 10
Moderately fouled	9.5 to < 17.5	10 to < 20
Fouled	17.5 to < 34	20 to < 40
Highly fouled	≥ 34	≥ 40

## 6.2 Resistivity and Percentage Fouling

The values of resistivity of fouled ballast are plotted against time in figures 5.3 and 5.4 for different percentages of fouling with crushed ballast and clay fines. As expected, the resistivity decreased as the percentage of fouling increased. Values of resistivity decreased due to the increase in the amount of water retained as the percentage of fouling increased. As evident in figures 5.3 and 5.4, resistivity values were measured at short time intervals. The resistivity increased rapidly as the water drained out of the sample before stabilizing after few hours. A final reading was taken 23 hours after the sample had the opportunity to drain, which resulted in the high value shown at the end of each curve in figures 5.3 and 5.4. However, as the percentage of fouling increased, the resistivity values also increased to a lesser extent during the early times as the water drained out. This was due to a decrease in the rate of drainage, as shown in figure 5.3, for 40% and 50% fouling in the ballast. In addition, the reading taken after 23 hours for the samples with 40% and 50% fouling increased to a lesser extent compared with the samples with 20% and 30% fouling.

Moreover, the results of the resistivity test are consistent with the permeability trends, since the resistivity drops dramatically at 30% and 40% fouling, and the water drains out more slowly due to the low permeability of the sample at higher percentages of fouling.

As observed in figure 5.3, the curve of the 30% fouled sample showed a slight decrease in the resistivity values after three hours of testing, before increasing for the final reading. Similar behavior was observed for the clay samples, as shown in figure 5.4. According to Tagg, the resistivity will decrease as temperature increases (10). This effect was presented in a study by Samouelian, which stated that ion agitation increases with temperature, resulting in a decrease in electrical resistivity (14). All the tests shown in figure 5.3 were conducted in the open air outside

of the laboratory, where the weather varied during the day and night for each test; however tests were begun in the morning, so temperatures generally increased during the initial 6-10 hours of testing, before decreasing with nightfall.

Figure 5.4 presents the results of resistivity tests of fouled ballast with clay fines at different percentages. The patterns of resistivity vs. time were similar to ballast fouled with crushed ballast fines, with a decrease in resistivity occurring as percentage fouling increased. Tests of the 20%, 30%, and 40% fouling ballast were conducted in the open air outside of the laboratory, and measurements were taken for up to 18 hours. The sample with 50% fouling was conducted inside the laboratory due to extreme weather conditions. As evident in figure 5.4, the curve for 50% fouling shows a steady line for resistivity measurements, presumably because the sample was not affected by temperature. Overall, as the percentage of fouling increased, more water was retained due to the reduction in rate of drainage, which resulted in less permeable and resistive ballast.

Tables 5.3 and 5.4 present the range of resistivity measurements for each percentage fouling sample for crushed ballast fine and clay. The ranges for each sample are relatively small compared to the large differences in resistivity with changes in percent fouling. The absolute values and the trends present in tables 5.3 and 5.4 are also consistent with the reference values for clay, sand, and crystalline rocks reported in table 2.1.

Figure 5.6 and table 5.5 show a comparison between permeability and resistivity of fouled ballast at the 18<sup>th</sup> hour. Solid curves represent the permeability test results and the dotted curves represent the resistivity results. As evident in figure 5.5, the patterns are similar, and show that as percentage of fouling increased, permeability and resistivity decreased at a comparable rate and were clearly correlated with each other and with fouling. This indicates that

measurements of either permeability or resistivity could be used to estimate the degree of fouling.

## Chapter 7 Conclusions and Future Work

A test box was used to conduct laboratory tests at the University of Kansas on fouled ballast obtained from Gardner, Kansas. The tests measured the permeability and resistivity of ballast fouled with two different fouling materials. Each fouling material was mixed with clean aggregates to obtain 20%, 30%, 40% and 50% fouling by dry weight. Results from using both crushed ballast fines and clay as fouling material showed similar patterns in permeability and resistivity. Permeability of hydraulic conductivity of ballast decreased as the percentage of fouling increased. Resistivity decreases in a similar manner as the percentage of fouling increased. Fouling index was observed to be a better proxy for hydraulic conductivity than percent fouling, because fouling index better accounts for the type of fouling material.

This preliminary study represents the first step in attempting to evaluate the percentage of fouling in a ballast layer using resistivity and permeability methods. Relationships between permeability, resistivity, and fouling were identified during this study, which suggests the goal of using measurements of either resistivity or permeability as a proxy for fouling may be successful. Further studies and test modifications are underway to fully understand these relationships. Future tests will include monitoring of sample temperatures to relate temperature to changes in resistivity values. Furthermore, strength tests will be performed on samples to evaluate the effect of different types and amounts of fouling on ballast strength.

## References

1. Indraratna, B., H. Khabbaz, W. Salim, and D. Christie. 2006. "Geotechnical properties of ballast and the role of geosynthetics in rail track stabilisation." *Ground Improvement*, 10, no. 3: 91-101.
2. Indraratna, B., W. Salim, and C. Rujikiatkamjorn. 2011. *Advanced rail geotechnology – Ballasted track*. University of Wollongong, Australia: CRC Press.
3. Huang, H., E. Tutumluer, and W. Dombrow. 2009. "Laboratory characterization of fouled railroad ballast behavior." *Transportation Research Record*, 2117: 93-101.
4. Roberts, R., and J. Rudy. 2006. "Railroad ballast fouling detection using ground penetrating radar. A new approach based on scattering from voids." *ECNDT 2006 – Th.4.5.1*. <http://www.ndt.net/article/ecndt2006/doc/Th.4.5.1.pdf>
5. Selig, E.T, and J. Waters. 1994. *Track geotechnology and substructure management*. London: Thomas Telford.
6. Raymond, G. P. 1978. "Design for railroad ballast and subgrade support." *Journal of the Geotechnical Engineering Division*, 105, no. 1: 45-60.
7. Wallace, A. J. 2003. "Permeability of fouled rail ballast." UG Thesis, School of Civil, Mining and Environmental Engineering, University of Wollongong, New South Wales, Australia.
8. Chiang, C. C. 1989. "Effects of water and fines on ballast performance in box tests." *Master of Science Degree Project Report No. AAR89-366P*. University of Massachusetts, Amherst, MA.
9. Han, X., and E. T. Selig. 1997. "Effects of fouling on ballast settlement." *Proceedings of the 6th International Heavy Haul Railway Conference*, Cape Town, South Africa.
10. Tagg, G. F. 1964. *Earth resistances*. Great Britain: Pitman Publishing Corporation.
11. AEMC Instruments. 15 Faraday Drive. Dover, NH.  
<http://www.aemc.com/products/html/minindex.asp?id=50306&dbname=products>
12. Ebrahimi, A., D. Fratta, and J. Tinjum. 2008. "Detection of fouling in ballast by electromagnetic survey." *Research in Nondestructive Evaluation*, 19, no. 4: 219-237.
13. Feldman, F. and D. Nissen. 2002. "Alternative testing method for the measurement of ballast fouling: Percentage voids contamination." *Proceedings of the Conference on Railway Engineering, Wollongong, Australia*. Railway Technical Society of Australia, Canberra, Australia, 101-109.

14. Jowkar, M. 2011. "Performance of geogrid reinforced ballast under dynamic loading." MS Thesis, CEAE Department, University of Kansas, Lawrence, KS.
15. Anbazhaga, P., B. Inraratna, C. Rujikiatkamjorn, and L. Su. 2010. "Using a seismic survey to measure the shear modulus of clean and fouled ballast." *Geomechanics and Geoengineering: An International Journal*, 5, no. 2: 117-126.
16. Leng, Z, and I. Al-Qadi. 2010. "Railroad ballast evaluation using ground penetrating radar: Laboratory investigation and field evaluation." *Transportation Research Record: Journal of the Transportation Research Board*, 2159: 110-117.
17. Samouelian, A., I. Cousin, A. Tabbagh, and Richard G. Bruand. 2005. "Electrical resistivity survey in soil science." *Soil & Tillage Research*, 83: 173-193.